In Situ Calibration of Optode-Based Oxygen Sensors

HIROSHI UCHIDA, TAKESHI KAWANO, IKUO KANEKO,* AND MASAO FUKASAWA

Institute of Observational Research for Global Change, Japan Agency for Marine-Earth Science and Technology, Yokosuka, Kanagawa, Japan

(Manuscript received 9 January 2007, in final form 12 April 2008)

ABSTRACT

Eleven optode-based oxygen sensors were used for shipboard hydrographic casts in the North Pacific. Oxygen data from the optode sensors were compared with high-quality oxygen data obtained with discrete water samples, and the performance of the sensors was evaluated. The response of the sensing foil of the optode decreases with increasing ambient pressure, and this pressure effect was found to decrease the response by 3.2% $(1000\ \text{dbar})^{-1}$. A new calibration equation for the optode sensors was proposed. On the basis of oxygen data from water samples, the optode sensors were calibrated so that the reproducibility was less than 1%. High-quality oxygen profiles from the optode were obtained for fast-profiling conductivity–temperature–depth (CTD) observations, by compensating for the temperature-dependent delay in the optode data due to the slow response time of the optode.

1. Introduction

Recent observational and model studies have consistently indicated that the oceanic oxygen inventory is decreasing owing to global warming. Keeling and Garcia (2002) have suggested that the global oceanic oxygen inventory may decrease by 0.7 μmol kg^{-1} decade^{-1} over the next few decades, if the decrease were distributed uniformly over 2000 m of the upper ocean, due mainly to the effect of warming on stratification and hence ventilation of the ocean. If changes this small are to be detected, high-quality oxygen data for the global ocean must be accumulated. In the 1990s, high-quality global hydrographic data were gathered as part of the World Ocean Circulation Experiment (WOCE) Hydrographic Program (WHP), and data quality goals were set (Joyce and Corry 1994). For conductivity–temperature–depth (CTD) oxygen data, the goal for both reproducibility and precision was set at 1%. To achieve this goal with the widely used polarographic oxygen sensor, cast-by-cast calibration during CTD observations is sometimes required because of sensor instability due to various phenomena (e.g., degradation of electrolyte, changing thickness and permeability of the membrane, and irreversible pressure effect).

Recently, an optode-based oxygen sensor has become commercially available for aquatic research (Tengberg et al. 2006). The optode-based measuring principle has various advantages: for example, the pressure behavior is fully reversible and predictable, no oxygen is consumed, and the measurement principle suggests that the sensors should exhibit long-term stability. Körtzinger et al. (2005) reported the first oxygen measurements from profiling floats equipped with optode sensors. Kobayashi et al. (2006), however, reported large discrepancies (up to -40 μmol kg^{-1}) between the oxygen concentrations measured with profiling floats equipped with optode sensors and oxygen concentrations in discrete water samples obtained from nearby shipboard hydrographic casts.

Although polarographic oxygen sensors have been widely used in CTD observations and polarographic and optode oxygen sensors have begun to be used in profiling float observations, the use of oxygen data from the sensors has been limited because in situ calibration is rarely carried out for these oxygen sensors, except for high-quality hydrographic observations like

* Current affiliation: Global Environment and Marine Department, Japan Meteorological Agency, Tokyo, Japan.

Corresponding author address: Hiroshi Uchida, Institute of Observational Research for Global Change, Japan Agency for Marine-Earth Science and Technology, 2-15 Natsushima, Yokosuka, Kanagawa 237-0061, Japan.
E-mail: huchida@jamstec.go.jp

DOI: 10.1175/2008JTECHO549.1

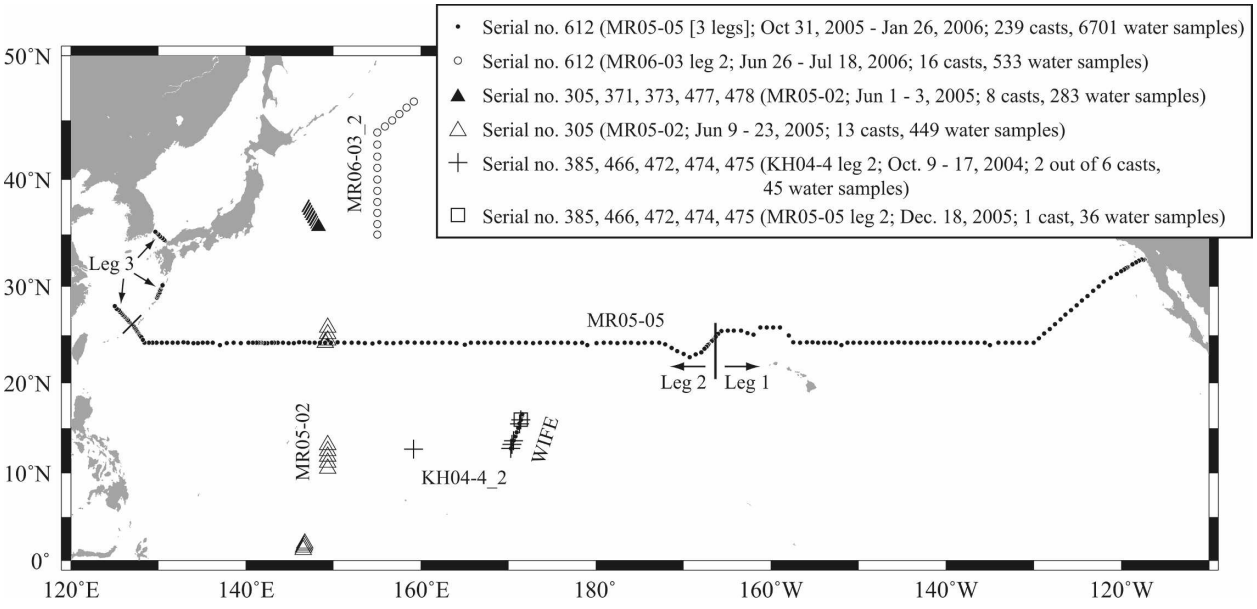

FIG. 1. Station locations of CTD casts for comparisons with 11 optodes. Cruise number, dates for CTD casts, number of CTD casts, and number of water samples are shown in parentheses. Five optodes (serial numbers 385, 466, 472, 474, and 475) were used in WIFE mooring observation (Uchida et al. 2007b) deployed in the cruise KH04–4 leg 2 and recovered in the cruise MR05–05 leg 2.

WHP. For example, continuous oxygen data from CTD and profiling floats were not used to calculate climatologies in the World Ocean Database 2005 (WOD05), owing to a low level of quality control (Boyer et al. 2006).

To obtain higher-quality data from oxygen sensors, the sensors should be calibrated using oxygen data from in situ water samples. Previously an in situ calibration procedure for polarographic oxygen sensors has been reported by Millard (1994), but few studies of in situ calibration for the new optode sensor have been done. In addition, for fast-profiling CTD observations (typical descent and ascent rates of 1 m s^{-1}), the optode sensor will develop a substantial disequilibrium owing to the relatively slow response time of the sensor. Tengberg et al. (2006) reported that the 67% response time was approximately 23 s at room temperature (~20°C) for optode sensors. However, they did not investigate the temperature dependence of optode sensor response time. Little information regarding the use of optode sensors for CTD observations has been published.

In this study, we evaluated the performance of 11 oxygen optode sensors based on comparisons with high-quality oxygen data obtained from discrete water samples. Using the oxygen data from the discrete water samples, we propose a new calibration equation for in situ calibration of optode sensors. We also introduce a method for compensating for the delay in optode oxygen data due to the slow response time of the sensors during fast-profiling CTD observation.

2. Materials and methods

Oxygen optode sensors (Oxygen Optode model 3830; Aanderaa Data Instruments AS, Bergen, Norway) are based on the oxygen luminescence quenching of a platinum porphyrine complex (Demas et al. 1999). The sensors have been described in detail by Körtzinger et al. (2005) and Tengberg et al. (2006). In this study, the model 3830 optode sensor was used in two configurations. In one configuration, the optode sensor was equipped with an analog adapter in a titanium housing designed for shipboard CTD observations. In the other configuration, the optode sensor was attached to a datalogger with an internal battery and memory in a titanium housing designed for mooring observation (Compact-Optode; Alec Electronics Co., Ltd., Kobe, Japan). The digital signal from the optode sensor was directly stored in the datalogger.

An analog optode was used in the R/V *Mirai* cruises MR05–05 and MR06–03 leg 2. Ten optodes designed for mooring observation were used: five in the R/V *Mirai* cruise MR05–02, and five in the R/V *Hakuhomaru* cruise KH04–4 leg 2 and in the R/V *Mirai* cruise MR05–05 leg 2. The second group of five was also used in the mooring observation of 14 months at about 5400-m depth deployed in the cruise KH04–4 leg 2 and recovered in the cruise MR05–05 leg 2. Station locations of CTD casts made with these optodes are shown in Fig. 1.

An SBE 9*plus* CTD system was used (Sea-Bird Elec-

tronics, Inc., Bellevue, Washington). The analog optode data (differential phase shift information) at a rate of 1 sample per second were transmitted from the underwater CTD unit in real time with CTD data at 24 samples per second. The optodes designed for mooring observation were attached to the CTD frame and lowered along with the CTD system, and temperature-comensated oxygen data along with temperature data were stored in the internal memory at a rate of 1 sample per second. From the oxygen and temperature data, phase shift data (typically between 10° and 70°) were back calculated and used with the CTD data with careful correction for differences between the time stamp for the CTD data and the time stamp for the optode data. Necessary temperature compensation for calculation of the optode oxygen data was performed using the high-quality CTD temperature data (both accuracy and precision have been estimated at 0.0004°C for depths deeper than 2000 dbar; Uchida et al. 2007a) instead of the less accurate temperature data from the slow-responding internal temperature sensor on the optode.

Because the sensing foil of the optode is permeable only to gas and not to water, the optode cannot sense the effect of salt dissolved in the water. Therefore, the optode sensor always measures as if it was immersed in freshwater. In addition, the response of the sensing foil decreases with increasing ambient pressure. Therefore, the temperature-compensated optode oxygen data were corrected for salinity and pressure using the CTD salinity and pressure data. The salinity compensation involved multiplying the oxygen data by the ratio of oxygen saturation at the observed salinity to oxygen saturation at the optode's internal salinity setting. The oxygen saturation values were calculated as a function of salinity and temperature, following García and Gordon (1992). The pressure compensation was done according to the procedure described in the operating manual for the model 3830 optode sensor, with a slight modification. Details of the pressure compensation procedure are described in section 4.

The CTD package was stopped at several water sampling levels (a maximum of 36 levels for the R/V *Mirai* cruises and of 24 levels for the R/V *Hakuho-maru* cruise) on the upcast for collection of a water sample. The water sample bottle was closed 30 s after the stop. The CTD and optode data were averaged over 4.4 s after the bottle was closed, for comparison with oxygen concentrations from the water samples.

Error of the optode data due to the slow response time was estimated from the water sample data obtained in the MR05–05 and MR06–03 leg 2 cruises. The maximum vertical gradient of oxygen concentration was 250 μmol kg^{-1} 50 dbar^{-1}. It usually took 2 min for the CTD package to travel a distance of 50 dbar between two sampling layers. Assuming the optode sensor was in equilibrium at the lower sampling layer and a response time (*e*-folding time) of the sensor was 21 s, the error of the optode data was estimated to be 50 μmol kg^{-1} when the CTD package stopped at the upper sampling layer. Since the water sample bottle was closed 30 s after the stop, the error was reduced to 12 μmol kg^{-1}. In addition, the difference of the vertical position (about 0.5 m) between the water sample bottles and the CTD could cause a discrepancy (2.5 μmol kg^{-1}) between the water sample data and the optode data. Though the maximum error (14.5 μmol kg^{-1}) was quite large, 95% of the observed oxygen gradient was smaller than one-tenth of the maximum, and the error was thus estimated to be generally smaller than 1.45 μmol kg^{-1}.

Oxygen concentrations in the water samples were measured by means of the Winkler titration method (Dickson 1996) using two sets of automatic photometric titrators (DOT-01; Kimoto Electronic Co., Osaka, Japan). Precision of the Winkler oxygen data was evaluated from standard deviations (STDs) of replicate samples as less than 0.13 μmol kg^{-1} for the R/V *Mirai* cruises and 0.24 μmol kg^{-1} for the R/V *Hakuho-maru* cruise. The Cooperative Study of the Kuroshio and Adjacent Regions (CSK) Standard Solution Potassium Iodate (Wako Pure Chemical Industries, Ltd., Osaka, Japan) were measured on each cruise to estimate the reproducibility of oxygen analyses between the cruises. The maximum difference from the certified value (0.0100 N) was 0.1% for 36 measurements. Actually, the mean oxygen difference between the cruise MR05–05 leg 2 and KH04–4 leg 2 was small (-0.33 μmol kg^{-1} or -0.2%) for the abyssal water of the Wake Island Passage Flux Experiment (WIFE) section (Fig. 1) (Uchida et al. 2007b). High-quality Winkler oxygen data were obtained during the cruises (Fig. 2) and used for in situ calibration of the optode sensors. The water samples were taken from depths ranging from 3 to 6505 dbar, and the oxygen concentration range of the data was 9–341 μmol kg^{-1}.

3. Comparisons with Winkler oxygen

First we will describe the procedures for manufacturer and user calibration of the optode in the laboratory. Oxygen concentrations [O_2] in μmol L^{-1} are calculated from the optode data by means of a fourth-order polynomial:

$$[O_2] = C_0 + C_1P + C_2P^2 + C_3P^3 + C_4P^4, \quad (1)$$

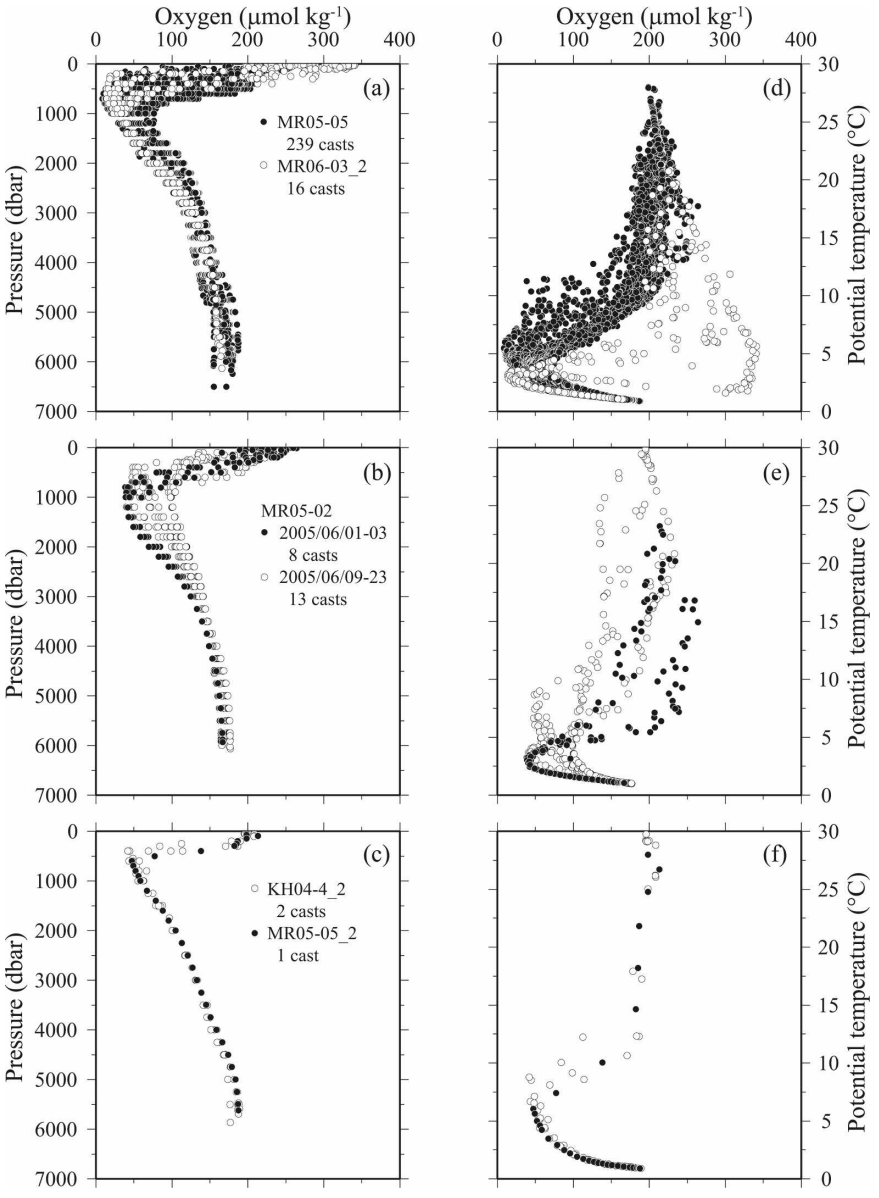

FIG. 2. Winkler oxygen data from discrete water samples used for the comparisons with optodes plotted against (left) pressure and (right) potential temperature. Data for (a), (d) 1 analog optode (serial number 612), (b), (e) 5 optodes (serial numbers 305, 371, 373, 477, and 478), and (c), (f) 5 different optodes (serial numbers 385, 466, 472, 474, and 475).

where P is the phase shift in degrees, and C_X ($X = 0, 1, 2, 3, 4$) are temperature-dependent coefficients calculated from the following equation:

$$C_X = C_{X0} + C_{X1}t + C_{X2}t^2 + C_{X3}t^3, \qquad (2)$$

where t is temperature in degrees Celsius. The 20 temperature-dependent coefficients (C_{XY}, where $X = 0, 1, 2, 3, 4$ and $Y = 0, 1, 2, 3$) are determined for 4 randomly selected foils in each batch of 100 sensing foils by a 35-point calibration (five temperatures and seven oxygen concentrations), and then the 4 sets of coefficients are averaged to obtain a representative set of coefficients. A calibrated phase shift (P_c) was determined for each optode sensor: $P_c = A + BP_r$, where P_r is the raw phase shift, and A and B are coefficients determined by a two-point calibration using 100% saturated with air solution and 0% oxygen solution. The optode oxygen values are calculated from Eq. (1) using the calibrated phase shift. These A and B coefficients were determined by the manufacturer (Aanderaa Data Instruments AS)

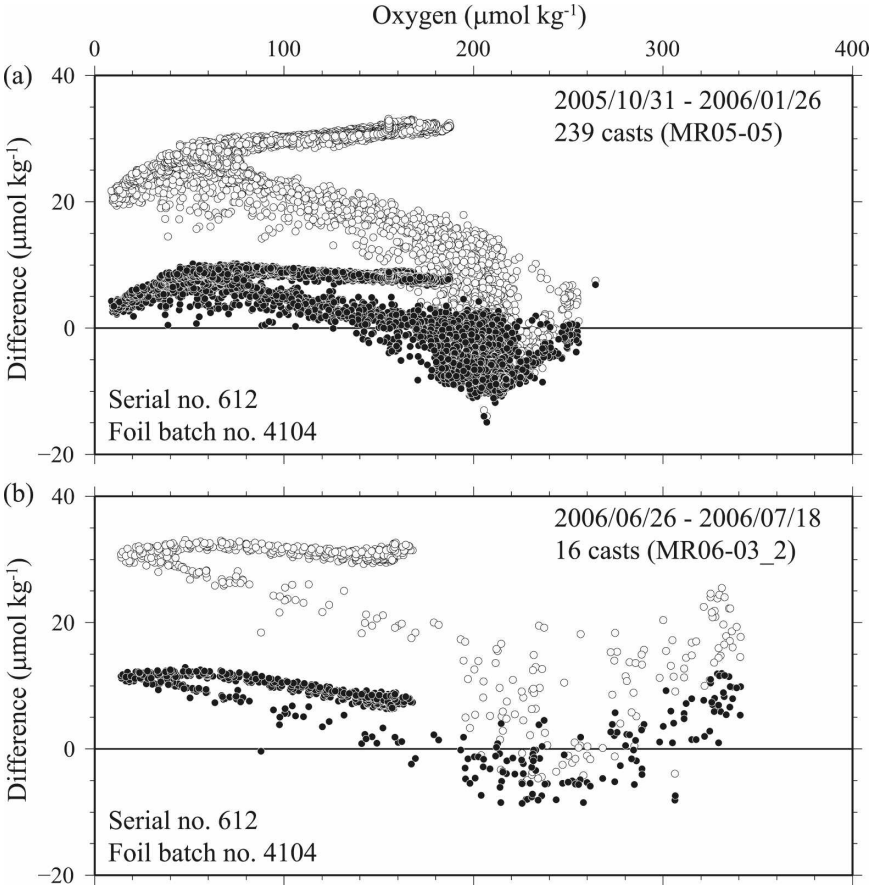

FIG. 3. Difference between oxygen data from the analog optode and Winkler oxygen data plotted against Winkler oxygen data for (a) cruise MR05–05 and (b) cruise MR06–03 leg 2. Filled circles show optode oxygen values calculated with Eq. (1) using the calibrated phase shift obtained by the two-point calibration, and open circles show optode oxygen values calculated with Eq. (1) using the raw phase shift.

and delivered with the sensor. For the optodes with serial numbers 305, 371, 373, 477, and 478, the two-point calibrations were performed by Alec Electronics.

The optode oxygen data obtained with the analog optode were compared with the Winkler oxygen data (Fig. 3). For the comparisons, the optode oxygen data in volumetric unit (μmol L^{-1}) were converted to gravimetric unit (μmol kg^{-1}) by dividing by water potential density. The differences between the optode and Winkler oxygen data were smaller at the oxygen minimum layer (near-zero oxygen concentration) and in well-oxygenated surface waters (Fig. 3a) when the two-point calibration was performed about 1 month before the optode was used. However, systematic differences up to about ± 10 μmol kg^{-1} existed. The differences observed during the MR06–03 cruise (Fig. 3b) were larger than the differences observed during the MR05–05 cruise (Fig. 3a) (by about $+5$ μmol kg^{-1} near the oxygen minimum layer). This change between the two cruises likely came from the optode data, because reproducibility of the Winkler oxygen data was much smaller than the change (section 2). We believe that the optode readings from the MR06–03 cruise did not drift linearly over time but rather were biased between the two cruises, because such a large drift (5 μmol kg^{-1} over a period of 5 months) was not observed in the readings from the MR05–05 cruise (Fig. 3a) during the 2.5-month observation period. This shift of the optode data is discussed in section 5.

The optode oxygen data from the 10 optodes designed for mooring observation were also compared with the Winkler oxygen data (Fig. 4). As for the analog optode oxygen data, the differences were smaller at zero oxygen concentration (as indicated by linear extrapolation of the trend for the oxygen difference below 150 μmol kg^{-1} to zero oxygen concentration) and at the surface when the two-point calibration was performed within 5 months before use of the optodes. However,

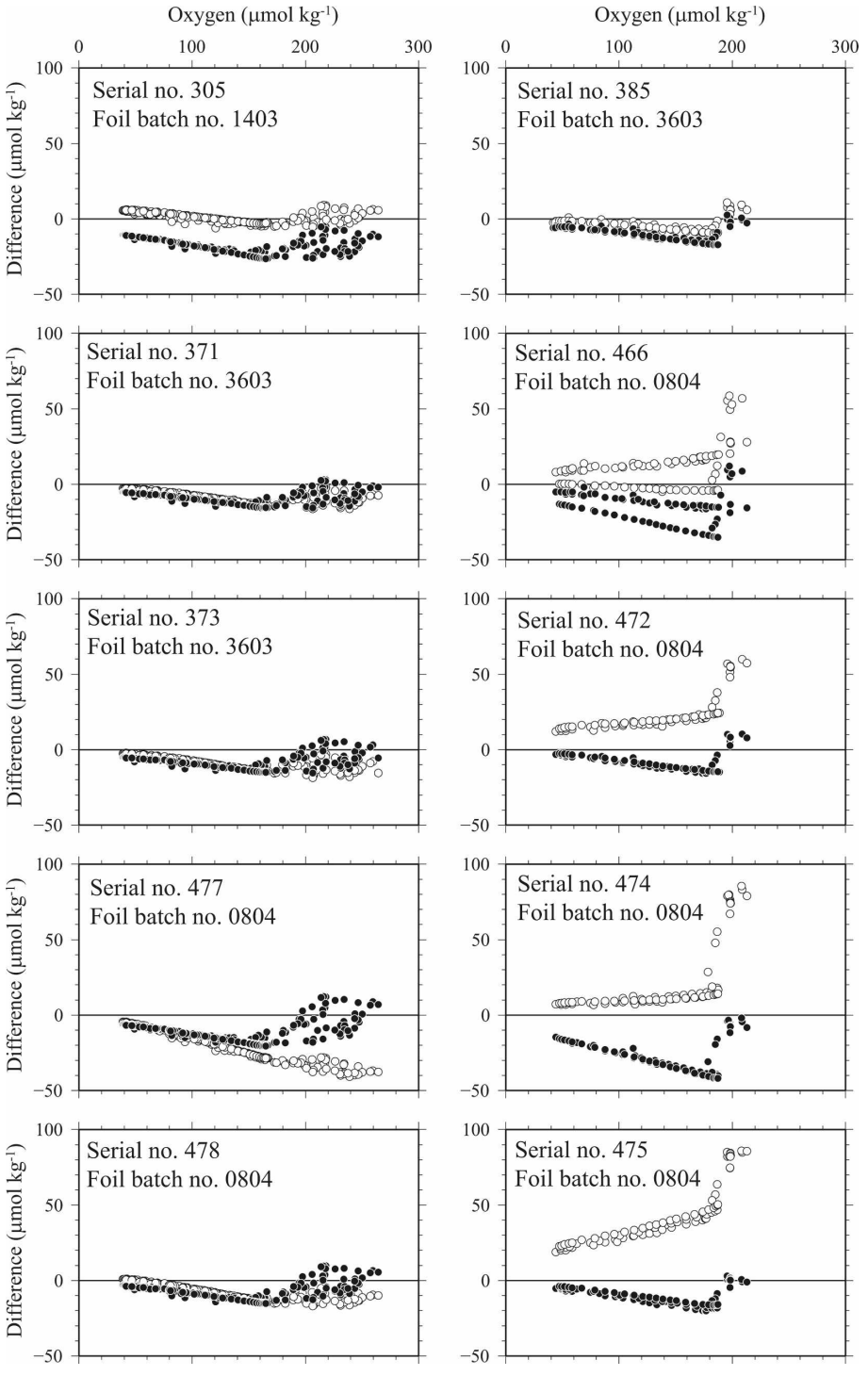

FIG. 4. Difference between oxygen data from 10 optodes designed for mooring observation and Winkler oxygen data plotted against Winkler oxygen data for (left) cruise MR05–02 and (right) cruise KH04–4 leg 2 and MR05–05 leg 2. Filled circles show optode oxygen values calculated with Eq. (1) using the calibrated phase shift obtained by the two-point calibration, and open circles show optode oxygen values calculated with Eq. (1) using the raw phase shift.

there were systematic differences (up to −40 μmol kg^{-1}) that were considerably beyond the nominal accuracy (±5% or ±8 μmol L^{-1}—whichever is greater; Aanderaa Data Instruments AS). The systematic differences tended to be negative for these 10 optodes, whereas the systematic differences for the analog optode tended to be positive.

Long-term stability was found to be an advantage of the optodes, as indicated by comparisons of the data for the five optodes (right panels in Fig. 4) before and after 14 months of mooring observations. The difference between the readings obtained from the optodes before and after the mooring observations was estimated to be less than 2.4 μmol kg^{-1} at 190 μmol kg^{-1} (approximate oxygen concentration at moored depth), except for optode serial number 466, the readings of which decreased by 21 μmol kg^{-1}. Readings from the irregular optode sensor (serial number 466) during the mooring observation showed a similar large drift (−17 μmol kg^{-1} over 2.5 months), although data were obtained only for the first 2.5 months because of a failure of Alec Electronics's firmware. The cause of the large drift has not been determined, despite a close examination of the sensor by Aanderaa Data Instruments AS.

The systematic differences between the optode oxygen data and the Winkler oxygen data showed no linear bias against oxygen concentration (Figs. 3, 4). The results suggest that the laboratory calibration procedure (calibration for each batch of foils and two-point calibration for each sensor) was insufficient for achieving the WHP goal for reproducibility (1%) with the optode sensors. That is, the sensor response should be fitted against oxygen concentration not for each batch of foils but for each optode sensor.

4. In situ calibration

The oxygen optode sensors were calibrated by adjusting the seven coefficients (C_{01}, C_{02}, C_{03}, C_{04}, C_{11}, C_{12}, and C_{21}) in Eq. (2), instead of applying the result of the two-point calibration. When there are outlier points to a Gaussian model for experimental error, the method of minimizing the mean absolute deviation is more robust than the method of minimizing the mean square deviation (Press et al. 1992). Therefore, the in situ calibration coefficients were determined by minimizing the mean absolute deviation from the Winkler oxygen data by means of the revised quasi-Newton method (the FORTRAN subroutine DMINF1 from the Scientific Subroutine Library II, Fujitsu Ltd., Kanagawa, Japan). This in situ calibration method provided sufficiently accurate calibration results for the WHP goal for reproducibility (1%), when the pressure compensation was performed as described below. The coefficient of variation (CV) was 0.6% for pressure <1000 dbar and 0.4% for pressure ≥1000 dbar (Fig. 5b).

The response of the sensing foil decreases with increasing ambient pressure. Using pressure cycling tests between 30 and 4050 dbar, Tengberg et al. (2006) suggested that the pressure effect decreases the response by 4% per 1000 dbar. Therefore, the pressure-compensated oxygen concentration $[O_2]_c$ can be calculated from the following equation: $[O_2]_c = [O_2](1 + C_p p/1000)$, where p is pressure in dbar and C_p is the compensation coefficient. When the suggested value (0.04) for C_p was used, however, the average difference between the optode oxygen data and the Winkler oxygen data deviated from zero below 4000 dbar (Fig. 5a). By minimizing the deviation, we empirically determined the best choice for the C_p value to be 0.032 (Fig. 5b), and this value was used in this study.

Although the calibration method described above gave us sufficiently accurate results, the calibration equation [(1)] is not theoretical but fully empirical, and the in situ calibration method is somewhat artificial because only 7 out of 20 coefficients are adjusted. Therefore, we propose a new formula to calculate oxygen concentration from phase shift data of an optode sensor, on the basis of the theoretical relationship between oxygen concentration $[O_2]$ and luminescence decay time (τ), as follows: $[O_2] = (\tau_0/\tau - 1)/K_{sv}$, where τ_0 is the decay time in the absence of $[O_2]$, and K_{sv} is the Stern–Volmer constant (Tengberg et al. 2006). The ratio τ_0/τ is replaced with the ratio of the phase shift P_0/P_c, where P_c is the corrected phase shift and P_0 is the phase shift in the absence of $[O_2]$, because the phase shift is a function of the decay time and the ratio P_0/P_c was more linearly related to $[O_2]$ than the ratio τ_0/τ calculated from the phase shift data (P) using the following relation: $\tau_0/\tau = \tan(P_0)/\tan(P)$ (Demas et al. 1999) (Fig. 6). Because both τ_0 and K_{sv} may be expressed as a function of temperature (Sinaasappel and Ince 1996), the oxygen concentration $[O_2]$ can be calculated from the phase shift by means of the following equations:

$$[O_2] = (P_0/P_c - 1)/K_{SV}, \tag{3}$$

and

$$K_{SV} = c_0 + c_1 t + c_2 t^2, \quad P_0 = c_3 + c_4 t, \quad \text{and}$$
$$P_c = c_5 + c_6 P_r, \tag{4}$$

where t is temperature in degrees Celsius, P_r is the raw phase shift in degrees, and c_x ($x = 0, 1, \ldots, 6$) are the calibration coefficients. The new formula gave us re-

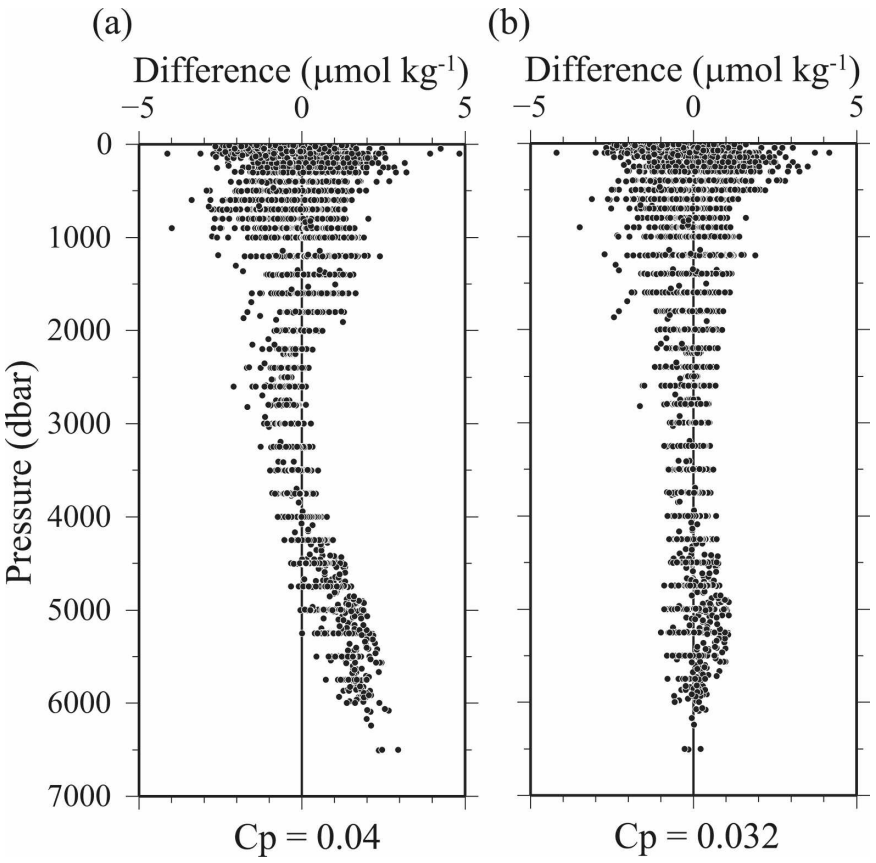

FIG. 5. Difference between in situ calibrated analog optode oxygen data and Winkler oxygen data plotted against pressure for cruise MR05–05 (6701 samples). The pressure compensation for the optode oxygen was performed using pressure compensation coefficients (C_p) of (a) 0.04 and (b) 0.032.

sults that were comparable to the results obtained from the in situ calibration method using Eq. (1).

The oxygen optode data were calibrated using the new formula [Eq. (3)] (Fig. 7). The calibration coefficients were determined for each cruise. For the MR05–05 cruise, however, the coefficients were determined individually for the two periods (leg 1 and leg 2–3), because the calibration results were slightly improved by this method. Moreover, for the MR06–03 cruise, the in situ calibration formula was slightly modified to obtain better calibration results. The offset (c_5) for the phase shift in Eq. (4) was changed for the three groups of CTD casts. This offset correction for the optode during the cruise is discussed in section 5. The systematic differences seen in the results from the manufacturer's calibration (Fig. 3) were almost eliminated when this method was used. In addition, one optode (serial number 305) for mooring observation, the data for which were obtained from a relatively large number of CTD casts, was calibrated (Table 1). The offset (c_5) was also changed for four groups of CTD casts. These optodes could be calibrated with sufficient reproducibility for the WHP goal (Table 1).

5. Discussion

a. Shift of the optode data

The results of the in situ calibration indicate that the response of the analog optode sensor seemed to change when the sensor was removed from the CTD system between leg 1 and leg 2 of the MR05–05 cruise, and between the MR05–05 and MR06–03 cruises. Moreover, for the in situ calibration in the MR05–02 and MR06–03 cruises, the offset corrections for the optode data for some groups of the CTD casts were effective. The shift of the optode data seemed to occur when the analog optode sensor was removed from the CTD system or when the optode for mooring observation was removed from the CTD frame for a change of the internal battery. The results of the in situ calibration showed that the optode data (phase shift) were de-

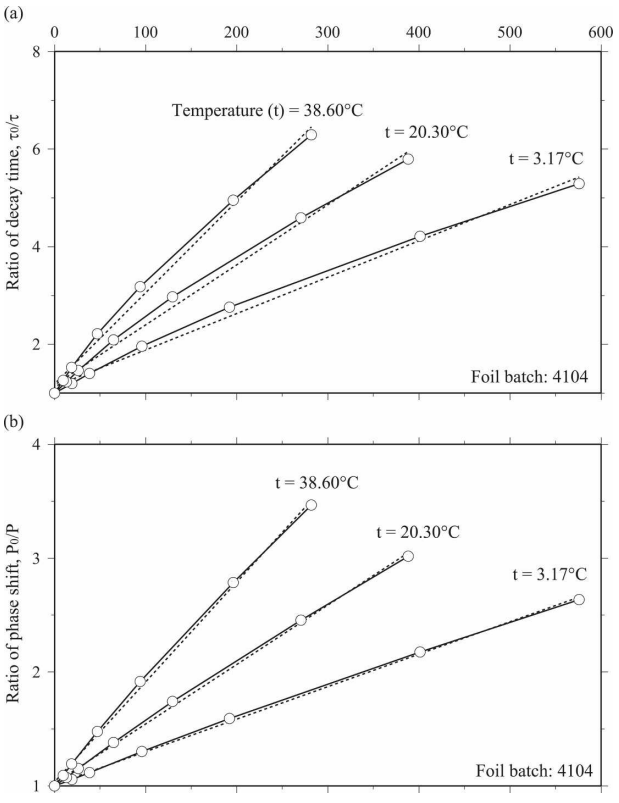

FIG. 6. Oxygen concentration (μmol L^{-1}) plotted against ratio of (a) decay time (τ_0/τ) and (b) phase shift (P_0/P). Results from the manufacturer's calibration for a batch of foil (number 4104) are shown. The dashed lines are the regression lines.

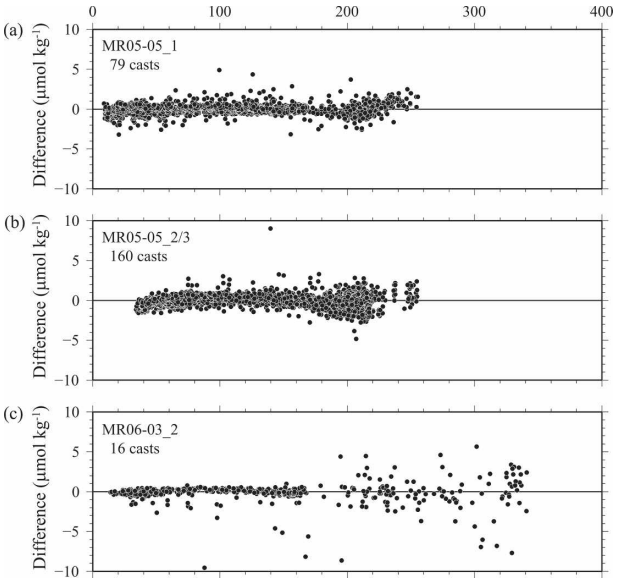

FIG. 7. Difference between oxygen data from the analog optode and Winkler oxygen data plotted against Winkler oxygen data. The optode oxygen data were calibrated in situ. A set of calibration coefficients was determined for the data obtained in the (a) MR05–05 leg 1, (b) MR05–05 legs 2 and 3, and (c) MR06–03 leg 2 cruises.

creased by about 0.07° for every shift during the cruises (MR05–02 and MR06–03).

Aanderaa Data Instruments AS has pointed out that a new two-point calibration must be done for an optode sensor if the foil has been moved because the response of the sensing foil to the oxygen concentration changes when the foil has been moved. The results of the in situ calibration suggest that the sensing foil might have been moved slightly when the optode sensor was removed from the CTD system for maintenance.

b. Data processing for profile data

For a fast-profiling CTD observation, differences between the downcast and upcast optode profile data can

TABLE 1. Summary of in situ calibration data for two optodes. STD of the difference between optode and Winkler oxygen data and CV are listed.

Serial No.	612	612	612	305
Cruise No.	MR05–05_1	MR05–05_2/3	MR06–03_2	MR05–02
Period of data	31 Oct–22 Nov 2005	30 Nov 2005–26 Jan 2006	26 Jun–18 Jul 2006	1–23 Jun 2005
No. of casts	79	160	16	21
For full depth				
No. of data	2332	4369	533	732
STD (μmol kg^{-1})	0.64	0.66	1.50	0.72
CV (%)	0.54	0.46	1.10	0.54
For pressure ≥1000 dbar				
No. of data	1319	2365	291	461
STD (μmol kg^{-1})	0.38	0.35	0.23	0.28
CV (%)	0.36	0.28	0.21	0.22
For pressure <1000 dbar				
No. of data	1013	2004	242	271
STD (μmol kg^{-1})	0.86	0.90	2.20	1.13
CV (%)	0.65	0.54	1.33	0.79

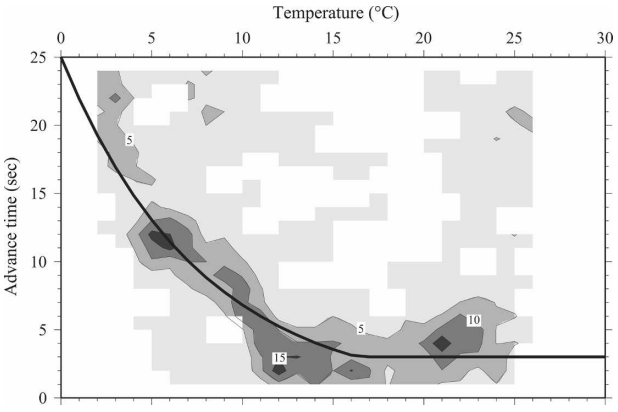

FIG. 8. Frequency (%) distribution of advance time, which minimizes discrepancies between the downcast and upcast optode oxygen data. The frequency distribution was calculated at 1°C intervals from the 181 CTD profiles obtained in the MR05–05 cruise. Line represents the function of T_a (see text for details).

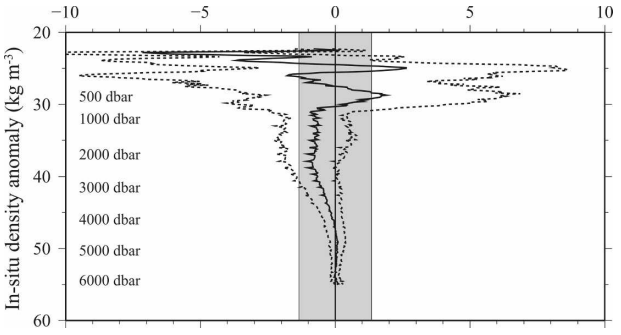

FIG. 9. Mean difference between downcast and upcast optode oxygen data from the analog optode plotted against in situ density anomaly derived from 255 CTD casts. Dashed lines represent 1 STD from the mean difference profile. Approximate pressures corresponding to the in situ densities are shown. The mean difference profile was within the WHP goal for reproducibility (1%) (gray shaded area) for depths deeper than 1000 dbar.

become large in a strong vertical gradient of oxygen, owing to the relatively slow response time of the optode sensors. Because typical descent and ascent rates were high (1.2 m s^{-1}) in our cruises, the optode data had to be aligned in time relative to the CTD data to account for the delay of the optode data due to the slow response time. The response time was likely to be affected by the ambient temperature from the profiles obtained in the MR05–05 cruise (Fig. 8). At temperatures below 10°C, the optode response time is probably much longer than the nominal value (23 s). Therefore, we compensated for the delay for optode serial number 612 by advancing the sensor output (phase shift) relative to the CTD temperature using the following functions: $T_a = 25e^{-0.13t}$ for $t < 16.3$ and $T_a = 3$ for $t \geq 16.3$, where T_a is advance time in seconds, and t is temperature in degrees Celsius. Discrepancies between the downcast and upcast profiles became smaller when compensation for the slow time response was applied (Fig. 9), although a systematic difference (about 1 μmol kg^{-1}) was seen at depths between 1000 and 3000 dbar. Each optode or sensing foil may have a somewhat different response time. Actually, the advance of 12 s for the other optode data resulted in less discrepancy between the downcast and upcast profiles. More work needs to be done to understand the individual sensors' response under various situations at ambient temperature and in a vertical gradient of oxygen for more accurate compensation of the profile data.

Acknowledgments. We thank Makio Honda and Shuichi Watanabe (JAMSTEC) for obtaining the optode data during the R/V *Mirai* cruise MR06–03. We also thank Yuichiro Kumamoto and Masahide Wakita (JAMSTEC) for analyzing the Winkler oxygen data from the R/V *Mirai* cruises. Comments by Taiyo Kobayashi (JAMSTEC) were helpful. We also thank Anders Tengberg (Göteborg University) and two anonymous reviewers for valuable comments, which improved the paper considerably.

REFERENCES

Boyer, T. P., and Coauthors, 2006: *World Ocean Database 2005*. NOAA Atlas NESDIS 60, U.S. Government Printing Office, 190 pp.

Demas, J. N., B. A. De Graff, and P. Coleman, 1999: Oxygen sensors based on luminescence quenching. *Anal. Chem.,* **71,** 793A–800A.

Dickson, A. G., 1996: Determination of dissolved oxygen in sea water by Winkler titration. WOCE operations manual, WHP operations and methods, WHPO 91-1, WOCE Rep. 68/91, WOCE International Project Office, 13 pp.

García, H. E., and L. I. Gordon, 1992: Oxygen solubility in seawater: Better fitting equations. *Limnol. Oceanogr.,* **37,** 1307–1312.

Joyce, T., and C. Corry, Eds., 1994: Requirements for WOCE Hydrographic Programme data reporting. WHPO 90-1, WOCE Rep. 67/91, WOCE International Project Office, 144 pp.

Keeling, R. F., and H. E. Garcia, 2002: The change in oceanic O_2 inventory associated with recent global warming. *Proc. Natl. Acad. Sci. USA,* **99,** 7848–7853.

Kobayashi, T., T. Suga, and N. Shikama, 2006: Negative bias of dissolved oxygen measurements by profiling floats (in Japanese). *Oceanogr. Japan,* **15,** 479–498.

Körtzinger, A., J. Schimanski, and U. Send, 2005: High quality oxygen measurements from profiling floats: A promising new technique. *J. Atmos. Oceanic Technol.,* **22,** 302–308.

Millard, R. C., Jr., 1994: CTD oxygen calibration procedure. WOCE operations manual, WHP operations and methods, WHPO 91-1, WOCE Rep. 68/91, WOCE International Project Office, 30 pp.

Press, W. H., S. A. Teukolsky, W. T. Vetterling, and B. P. Flannery, 1992: *Numerical Recipes in FORTRAN: The Art of Sci-*

entific Computing. 2nd ed. Cambridge University Press, 963 pp.

Sinaasappel, M., and C. Ince, 1996: Calibration of Pd-porphyrin phosphorescence for oxygen concentration measurements in vivo. *J. Appl. Physiol.,* **81,** 2297–2303.

Tengberg, A., and Coauthors, 2006: Evaluation of a lifetime-based optode to measure oxygen in aquatic systems. *Limnol. Oceanogr. Methods,* **4,** 7–17.

Uchida, H., K. Ohyama, S. Ozawa, and M. Fukasawa, 2007a: In situ calibration of the SeaBird *9plus* CTD thermometer. *J. Atmos. Oceanic Technol.,* **24,** 1961–1967.

——, H. Yamamoto, K. Ichikawa, I. Kaneko, M. Fukasawa, T. Kawano, and Y. Kumamoto, 2007b: Flow of abyssal water into Wake Island Passage: Properties and transports from hydrographic surveys. *J. Geophys. Res.,* **112,** C04008, doi:10.1029/2006JC004000.